

# Effect of clay content on electrostimulus deformation and volume recovery behavior of a clay–chitosan hybrid composite

Kun-Ho Liu, Ting-Yu Liu, San-Yuan Chen \*, Dean-Mo Liu

*Department of Materials Science and Engineering, National Chiao Tung University, 1001 Ta-hsueh Road, Hsinchu, Taiwan, China*

Received 27 February 2007; received in revised form 30 May 2007; accepted 11 June 2007

Available online 24 June 2007

## Abstract

Electrostimulus-responsive hybrid composites composed of chitosan (CS) and clay were successfully developed and systematically characterized. The addition of negatively charged clay as an ionic cross-linker strongly affect the cross-linking density as well as the mechanical property, swelling–deswelling behavior and fatigue property of the hybrids. With lower clay content, the crystallinity of the CS was slightly reduced, resulting in a decrease in the mechanical properties and an increase in the swelling ratio of the hybrid. However, the swelling kinetics were accelerated due to a reduction in CS crystallinity. On the other hand, with increasing clay concentration, the increased cross-linked bonding mechanically reinforced the hybrid beyond the aforementioned adverse effect, to show improved tensile strength and a decrease in the swelling ratio. The voltage-induced deformation of hybrids became more pronounced with increasing applied voltage, but became less pronounced with increasing clay content under an applied electric field. After repeatedly switching the electric field on and off, the higher clay concentration ( $C_{\text{clay}} > 0.5$  wt.%) of the hybrid composites maintained the same capability of deswelling and swelling after more than 10 cycles, compared with both the pure CS film and the hybrid composites with lower clay content (e.g., 0.5 wt.%). Compared with pure CS, a significant improvement in the anti-fatigue property against cyclic electric stimulations of the hybrid was found, which encourages the use of such a new class of hybrid composite in medical and pharmaceutical applications. © 2007 Acta Materialia Inc. Published by Elsevier Ltd. All rights reserved.

**Keywords:** Chitosan; Clay; Electric stimuli; Hybrid film; Anti-fatigue

## 1. Introduction

“Intelligent” or “smart” hydrogels which can control drug release by changing the gel structure in response to environmental stimuli have been used in diverse applications, such as artificial muscles [1], bioseparation [2] and drug delivery systems [3,4]. Environmental stimuli, such as pH, pressure, temperature, light, magnetic fields and electric fields, cause smart hydrogels to undergo macroscopic deformation and produce contractile force. Of those stimuli, the application of an electric field is one of the most frequently employed methods of triggering the desirable mechanical deformation of smart hydrogels for specific

engineering purposes. A typical example is artificial muscle, which can be applied directly as a medical device with a simple mechanical movement or employed as an electrically controllable matrix or switch for drug delivery in vitro and in vivo [5]. Using an electric field as an external stimulus has advantages, with the increased availability of equipment in the market that allows the precise control of a number of parameters, including the magnitude of the current, the duration of pulses and the intervals between pulses, which can be directly translated into precise deformation behavior of the hydrogels.

A significant drawback of most environmentally stimulus-sensitive hydrogels is that the responsivity and reversibility often decrease with both time and number of on–off operation cycles as the gel fatigues considerably. Generally, the deformation under a stimulus is increased with greater

\* Corresponding author. Tel.: +886 3 5731818; fax: +886 3 5725490.  
E-mail address: [sanyuanchen@mail.nctu.edu.tw](mailto:sanyuanchen@mail.nctu.edu.tw) (S.-Y. Chen).

molecular mobility in a gel of smaller cross-linking density. It is well known that the extent of gel deswelling increases with the magnitude of the electric voltage, but this increase is not linear. Gong et al. [6] reported that the extent of deswelling depended on the amount of charge transported through the gel, rather than on the voltage applied. Furthermore, after removal of the stimulation, volume recovery occurs because the gel absorbs fluid and swells, and this is also increased with low cross-linking density. Sutani et al. [7] reported that the differences, including cross-linking density, the mobility and flexibility of the network and the viscosity properties of the gel, might affect the deformation and relaxation properties of gel with cyclic on–off operations. At the same time, it was also proved that there is a most suitable composition and viscoelasticity at a certain cross-linking density for optimal electroresponsiveness. Shiga et al. found that an acrylacid–acrylamide gel swelled or deswelled under electrical stimulation, depending on the concentration of ions in the gel [8]. In order to further understand the dynamics of the ion species in ionic gels, Doi et al. [9] proposed a semi-quantitative theory to explain the swelling and shrinking (deswelling) behaviors of electroresponsive gels. However, the actual mechanism that causes the fatigue of the gel under stimulation is still not clear. Moreover, the fatigue problem of these hydrogels has to be circumvented to achieve the reliable performance required in medicine.

During the last decade, considerable attention was paid to inorganic–organic hybrid materials because their solid-state properties could be tailored in relation to the nature and relative content of their constitutive components. Low-volume additions (1–5 wt.%) of highly anisotropic nanoparticles, such as layered silicates, provide property enhancement with respect to the neat polymer that are comparable to those achieved by conventional loadings (15–40 wt.%) of traditional fillers. Besides, unique value-added properties not normally possible with traditional fillers are also observed, such as enhanced strength, electrical conductivity, electrostatic discharge, remote-actuated shape recovery and ablation resistance [10,11]. Wang et al. [12] successfully synthesized chitosan/montmorillonite nanocomposites and reported that nano-dispersed clay improved the thermal stability and enhanced the hardness and elastic modulus of the matrix systematically with increased clay loading, up to a loading of 10 wt.%. However, higher clay loading in the matrix could increase the possibility of inhomogeneous distribution of the clay. In this case, this increase in both hardness and elastic modulus of the chitosan/clay nanocomposite imparts sufficient rigidity to the nanocomposite. This will then deteriorate desirable flexibility of the composite upon controlled contraction–expansion deformation under environmental stimuli. Therefore, it is more technically interesting to prepare such a nanocomposite system which is flexible and mechanically strong enough to be operated reliably under cyclic environmental stimuli, such as electrical stimulation.

By taking advantage of the electrochemical properties, i.e., the surface charge, and nanostructural properties, i.e., the layer of the clay particles, a new class of electrically charged hybrid composites based on chitosan (CS) and clay was studied. The inorganic material, clay, used in this investigation is polysilicate magadiite ( $\text{Na}_2\text{Si}_{14}\text{O}_{29} \cdot n\text{H}_2\text{O}$ ), which is composed of one or multiple negatively charged sheets of  $\text{SiO}_4$  tetrahedra with an abundant silanol-terminated surface compensated by either  $\text{Na}^+$  or  $\text{H}^+$  in the inter-layer spacing. The cationic biopolymer chitosan, composed mainly of  $\beta$ -(1,4)-linked 2-deoxy-2-amino-D-glucopyranose units, is a deacetylated product of chitin. In the present study, with its incorporation into CS matrix, it is expected to enhance the thermal stability and mechanical properties of the resulting hybrid composites compared with neat CS polymer. Moreover, the electrically stimulated swelling–deswelling behavior, mechanical deformation and clay content of the hybrid composites will be elucidated.

## 2. Materials and methods

### 2.1. Materials

The chitosan used in this study to prepare the CS–clay nanocomposites was supplied by Aldrich–Sigma and used without purification. The same type of chitosan was used by Darder et al. [13], who found it to have an average molecular weight of  $342500 \text{ g mol}^{-1}$  and a deacetylation degree (DD) of  $\sim 75\%$ . Sodium phosphate for the preparation of buffers and acetic acid were purchased from Aldrich Chemicals. As inorganic clay, Na–magadiite was purchased from Chang-Chun Petrochemical Co. (Hsinchu, Taiwan). The mean particle size and size distribution of the clay were measured by an ultrafine particle size analyzer (Honeywell). The mean particle size of the clay (Na–magadiite) was estimated about  $3 \mu\text{m}$ , and a narrow particle size distribution of  $2\text{--}4 \mu\text{m}$  can be observed.

### 2.2. Preparation of CS–clay films

To prepare the CS–clay films, 1 g of CS was first dissolved in 40 ml of 1% acetic acid solution followed by centrifugation to remove the insoluble material. This ensures that the chitosan used to prepare the hybrid films can be completely dissolved without detectable insoluble fractions. Then, a small amount of clay (0.005, 0.01, 0.015, 0.02 and 0.03 g) was added to 10 ml of distilled water to form a suspension. Next, the mixed suspension added into the prepared CS solution with a clay content of 0.5, 1, 1.5, 2 and 3 wt.%, followed by stirring at  $60^\circ\text{C}$  until a uniformly distributed CS–clay suspension was obtained. This solution was then cast into Petri dishes (radius  $\sim 1.5 \text{ cm}$ ) and dried at  $30^\circ\text{C}$  for 24 h. The dried films were then immersed into an aqueous solution of 1 M NaOH to remove residual acetic acid. The obtained products were washed with distilled water and dried for 1 week at  $40^\circ\text{C}$  in vacuum.

### 2.3. Characterization

The crystal structures of hybrid films were determined using an X-ray diffraction (XRD) diffractometer (Siemens D5000) equipped with a Cu  $K\alpha$  radiation source ( $\lambda = 0.154$  nm). The diffraction data were collected from  $2\theta = 2 - 25^\circ$ . Fourier transform infrared (FTIR) spectra were recorded using a Bomem, DA8.3 FTIR spectrometer with attenuated total reflectance (Harrick). A Malvern Zetasizer HS3000 photon correlation spectrometer with an applied voltage of 100 V and a 5 cm quartz cell was used to determine the zeta potential values of clay (Na–magadiite) in phosphate-buffered solution (PBS) with different pH values (4, 6, 7 and 10). The concentration of clay in aqueous suspension was fixed at 0.1 wt.%. The tensile mechanical properties of the hybrid composites were measured using a complete MTS Tytron 250 and TestStar IIs system in the following conditions: crosshead speed,  $10 \text{ mm min}^{-1}$ ; test temperature,  $25^\circ\text{C}$ . The initial cross-section ( $10 \text{ mm}^2$ ) was used to calculate the tensile strengths and the tensile modulus. All results reflect the average of three measurements. The difference between each measurement is  $<5\%$ .

### 2.4. Swelling behavior of CS–clay films

The film was first cut into a circular plate (radius  $\sim 1$  cm). The average thickness and weight of the obtained dried films were measured to be  $\sim 0.20$  mm and 0.12 g, respectively. In order to measure the swelling ratio, each sample was weighed before and after immersion in PBS. After the excessive surface water had been removed with filter paper, the weight of swollen samples was measured at various time intervals. The procedure was repeated five times, until no further weight gain was detected. The swelling ratio was determined according to the following equation:

$$\text{Swelling ratio (\%)} = [(W_s - W_d)/W_d] \times 100$$

where  $W_s$  and  $W_d$  are the weights of the swollen and dried samples, respectively. All results reflect the average of five measurements. The difference between each measurement is  $<5\%$ .

### 2.5. Electrostimulus response behavior of CS–clay films

The film, pre-equilibrated and swollen in PBS, was cut into a circular plate (radius  $\sim 1$  cm) and weighed. Two platinum electrodes (radius  $\sim 1.5$  cm) were kept in contact with opposite surface of the film. The released water from the hybrid films was continually removed using filter paper and the weight change of the swollen hybrid films was checked periodically under an electric field. The deswelling water ratio was evaluated as  $W_t/W_{10}$  where  $W_{10}$  and  $W_t$  were the initial weight of the fully swollen films and the weight of films at deswelling time  $t$ , respectively. All results reflect the average of five measurements. The difference between each measurement is  $<5\%$ .

## 3. Results and discussion

### 3.1. Chemical interaction between the CS and the clay in the hybrid

Magadiite has a layered structure with negatively charged silicate layers compensated by interlayer sodium ions. The zeta potential profile in Fig. 1 shows the change of the electrical charge of the clay in buffer solution with different pH values. The isoelectric point of the clay was determined to be about 5.3, which indicates that above pH 5.3 the net charge of the clay is negative. The polycationic nature of CS makes it an excellent candidate for interaction with the negatively charged Na–magadiite clay by means of electrostatic attraction [14]. Thus, the clay in the CS matrix can act as an effective multi-functional cross-linker [15]. For this purpose, aqueous medium with a low pH value is employed to generate ionized  $-\text{NH}_3^+$  groups in the CS structure. An electrostatic attraction is expected to take place as a result of Coulombic interactions between the positively charged  $-\text{NH}_3^+$  groups of the CS and the negatively charged sites in the clay structure, which mainly controls the adsorption process. Fig. 2a shows the low-angle XRD patterns of the Na–magadiite, neat CS and CS–clay hybrid films. The  $d_{001}$  spacing is obtained using the first rational orders corresponding to the (001) reflection. From the XRD pattern of Na–magadiite, three reflection peaks can be observed at about  $2\theta = 5.63^\circ$ ,  $11.3^\circ$  and  $17.4^\circ$ , corresponding to the (001), (002) and (003) reflection planes. Herein, the peak at  $5.63^\circ$  corresponds to a basal spacing of 1.55 nm. After incorporating a small amount of the clay (1 and 2 wt.%), the basal plane of the clay at  $2\theta = 5.63^\circ$  disappeared, substituted by a new weakened broad peak at around  $2\theta = 8.1^\circ$ . The movement of the basal reflection of clay from  $2\theta = 5.63^\circ$  to  $8.1^\circ$  (the basal spacing = 1.1 nm) is believed to be a result of the replacement of  $\text{Na}^+$  by  $\text{H}^+$ . When the clay is placed in contact with acids, even weak and diluted acids, an exchange reaction of the interlayer sodium ions by protons takes

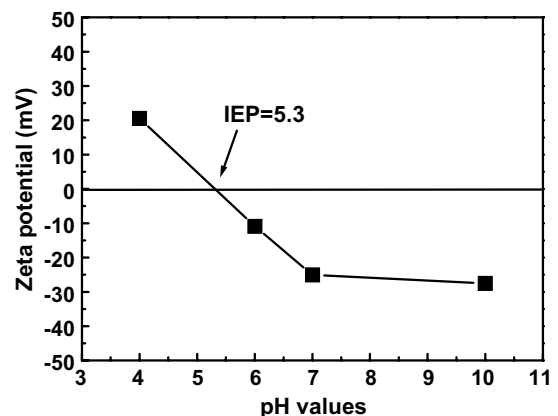


Fig. 1. Zeta potential profiles of nanoclay (magadiite) at various pH values.

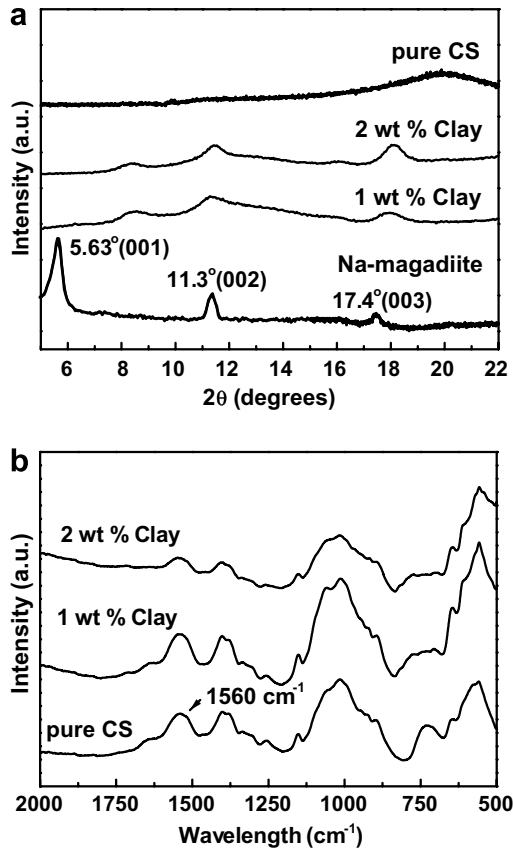


Fig. 2. (a) Low-angle powder XRD patterns and (b) FTIR spectra of hybrid films with various clay loadings.

place. It is believed that during the preparation of chitosan-based film, due to the presence of acetic acid, sodium ions are exchanged by protons, yielding the layered silicic acid called H-magadiite [16]. On the other hand, it is found that the intensity of the peak at  $2\theta \sim 20^\circ$ , which was identified as semi-crystalline CS, decreased with the incorporation of the clay. From the above results, it is believed that the dispersion of layer-type H-magadiite in the CS matrix may slightly deteriorate the crystallinity of CS. A further examination using IR spectroscopy reveals a strong absorption peak at  $\lambda = 1560 \text{ cm}^{-1}$ , which corresponds to the vibration of the protonated amine group ( $\delta_{\text{NH}_3^+}$ ) in CS and is broadened with the increase of clay addition (2 wt.%), as shown in Fig. 2b. This correlation strongly suggests that the  $-\text{NH}_3^+$  groups in the CS interacted electrostatically with the negatively charged sites of clay surface. This electrostatic interaction between the CS and the clay particles ensures the formation of bonding in between, which further generates a strong cross-linking structure in the final hybrid.

### 3.2. Degree of cross-linking in the hybrid

As negatively charged clay acts as an ionic cross-linker, the addition of clay will strongly affect the cross-linking density as well as the mechanical properties of the hybrids.

From mechanical properties, Fig. 3 shows that both the breaking tensile strength and the tensile modulus decreased slightly as 0.5 wt.% clay was added. However, both parameters improved with a further increase of clay concentration. The improvement in the mechanical properties was believed to be attributed to the formation of a higher population of CS–clay bonds in the hybrid and a more effective reduction in the molecular relaxation of the CS matrix. Therefore, it is reasonable to believe from the mechanical behavior of the hybrid composites that the negatively charged clay incorporated is able to form a physically strong network structure associated with the positively charged CS matrix. Furthermore, the cross-linking density, which is equivalent to the number of cross-linked chains per unit volume, is mainly determined by the concentration of CS polymer and the initiator at a fixed amount of clay. The number of cross-linked polymer chains per unit volume of the hybrid,  $N^*$ , can be estimated according to Eq. (1) [17] by using the stress at 100% elongation ( $\alpha = 2$ ):

$$F = \Phi N^* kT \left\{ \alpha - \left( \frac{1}{\alpha} \right) \right\} \quad (1)$$

here,  $F$  is the force per unit original cross-sectional area of the swollen network,  $\Phi$  is a front factor ( $=1$ ),  $\alpha$  is the elongation ratio, and  $k$  and  $T$  are Boltzmann's constant and the absolute temperature. The data,  $N^*$ , measured from Eq. (1) with different concentrations of clay ( $C_{\text{clay}}$ ) are illustrated in Fig. 4. At lower clay content (e.g. 0.5–1 wt.%), it was observed that the value of  $N^*$  of the hybrids was less than that of the pure CS. This lower cross-linking density of the hybrids is most probably due to its lower crystallinity. As evidenced from the XRD results (Fig. 2a), it was

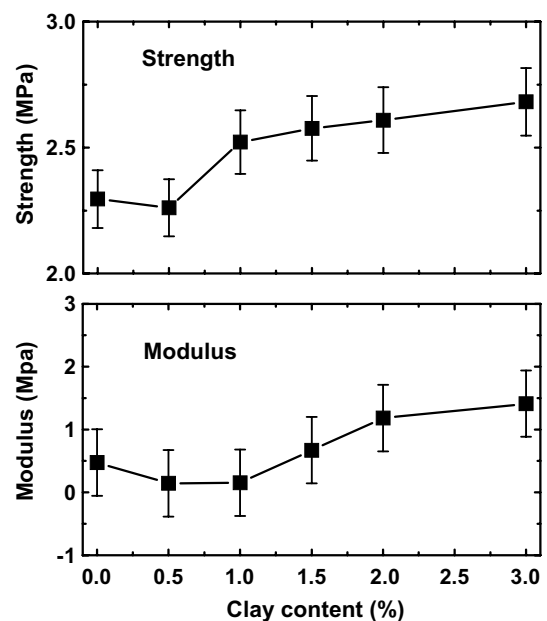


Fig. 3. Mechanical properties of hybrid film. The initial cross-sectional area ( $10 \text{ mm}^2$ ) was used for calculating the modulus and strength.

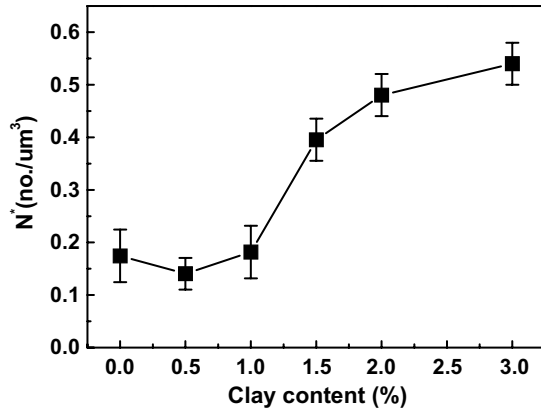


Fig. 4. Clay content dependencies of the number of cross-linked chains ( $N^*$ ).

demonstrated that the incorporation of clay would slightly deteriorate the crystallinity of CS. However, at the same time, increasing the clay in the CS matrix will also provide more chemically cross-linked bonds between the CS and clay, resulting in a more pronounced improvement in the mechanical properties. As clay is incorporated, competition arises between the deterioration of CS crystallinity and the increase in cross-linking density that dominates the performance of the resulting hybrid composites. With further increasing clay concentration, the increased cross-linked bonds reinforce the hybrid over the adverse effect with only a small addition of clay. Thus, the number of cross-linked polymer chains per unit volume ( $N^*$ ) is increased with increasing  $C_{\text{clay}}$ , wherein improved physical properties can then be expected.

Accordingly, it is of great interest to explore the swelling and deswelling behavior of this new class of hybrids, and in particular the improved anti-fatigue properties under cyclic electrostimulations.

### 3.3. Swelling–deswelling behavior of the hybrid films

It is well known that positively charged CS at low pH exhibits a high swelling ratio due to the repulsive force between the same positively charged molecules, which would result in longer intermolecular distance and more hydrophilic property. In other words, increasing the pH of the solution will reduce the repulsion force, thus further limiting the hydration of the CS. The swelling kinetics at PBS (pH 7.4) of pure CS and hybrid film with different  $C_{\text{clay}}$  are displayed in Fig. 5a. It should be noted that the swelling equilibrium was reached rapidly (within 20 min) at pH 7.4. Reaching an equilibrium state in such a short time period was helpful for further cyclic swelling and deswelling tests.

In order to gain a better understanding of the effect of clay on the swelling behavior of the composites, plots of  $\ln(W_0/W_t)$  against time after the initial 10 min are illustrated in Fig. 5b. All plots show straight lines, indicating that the process of the swelling may be illustrated by

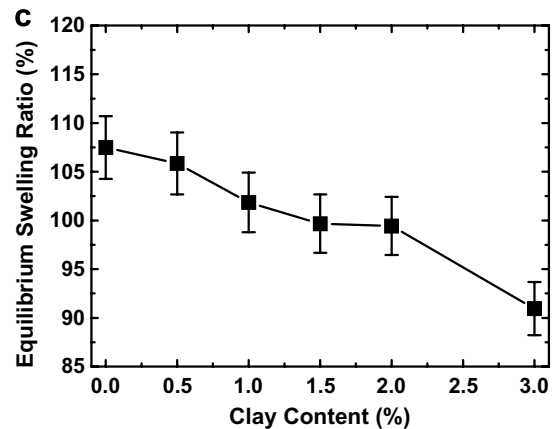
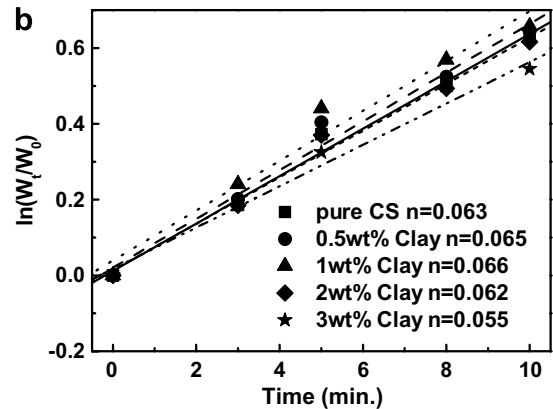
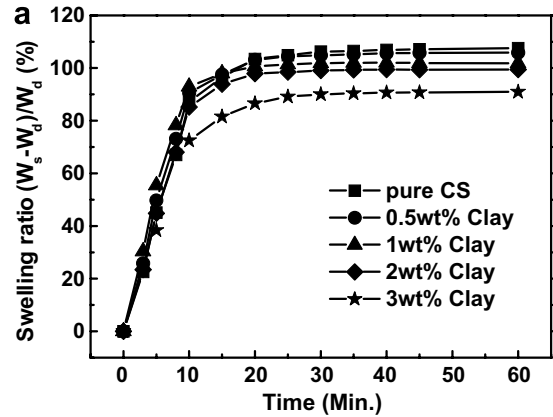


Fig. 5. (a) Swelling kinetics, (b) plots of  $\ln(W_0/W_t)$  against time and (c) equilibrium swelling ratio of hybrid film with different  $C_{\text{clay}}$  at pH 7.4.

apparent first-order kinetics as described by the pseudo-first-order kinetic equation [18]:

$$\ln\left(\frac{W_0}{W_t}\right) = nt + k \quad (2)$$

where  $W_0$  and  $W_t$  are the weights of the hybrid composites at  $t = 0$  and any time  $t$ , respectively,  $n$  is the first-order rate constant ( $1 \text{ s}^{-1}$ ) and  $k$  is a constant. Evidently, the linear fitting showed a reasonably good correlation (with a correlation coefficient,  $r^2 = 0.9862$ ). It can be seen that the value of the first-order rate constant  $n$  showed a small increase,

compared with the pure CS, from 0.063 to 0.066 as a small amount of clay was added (0.5–1 wt.%). However, when the amount of the clay increased above 3 wt.%, the high cross-linking degree decreased the swelling rate, resulting in a greater decrease in  $n$  value ( $n = 0.054$ ). In addition, the equilibrium swelling ratios of the composites are also affected by the incorporation of the clay. As seen from Fig. 5c, the equilibrium swelling ratio of the composites reduced from 106% to 91.0% with the increase of clay from 0 to 3 wt.%. The decrease in the equilibrium swelling ratio with increasing  $C_{\text{clay}}$  was also observed at pH 4 and 10 (not showed here). This result can be attributed to either a reduced number of functional groups or a proportional reduction in ionizable functional groups in the CS as a result of extensive cross-linked bonding formed between the positively charged CS and the negatively charged clay. From the above results, the swelling behavior of chitosan film does not differ substantially from that of the hybrid films with 0–2 wt.% clay contents. For example, when a small amount of clay was added (0.5–2 wt.%), the value of  $n$  and equilibrium swelling ratio was calculated to lie between 0.063 and 0.062 (106% and 102%), respectively. However, the hybrid film with 3 wt.% addition of clay does show a larger difference in the swelling kinetics and equilibrium swelling ratio compared with other samples, i.e.,  $n = 0.054$  and 91.0%, respectively. This suggests that as the clay concentration exceeds a critical concentration, an effective cross-linked interaction between the surface of clay particles and the chitosan molecular chain can be efficiently developed. Hence, high cross-linking density caused by a higher  $C_{\text{clay}}$  (3 wt.%) decreased both the swelling rate and the equilibrium swelling ratio.

CS is a cationic biopolymer and has been proposed for electrically modulated drug delivery [19]. Its deswelling behavior is critical for the reliable performance of a number of biomedical applications, such as drug delivery, wherein a release rate can be controlled externally or internally from slow to pulsatile release profiles according to practical needs. The mechanism of the deswelling behavior is generally thought to be the macroscopic contractile deformation of a polymer hydrogel under an electric field. This is due to the voltage-induced movement of ions across the entire polymeric matrix and the concomitant expansion on one side and contraction on the other side of the polymer [8]. Fig. 6a exhibits the deswelling ratio as a function of time with different applied voltages and clay concentrations. The deswelling rate of the composites was enhanced in proportion to the applied voltage, which suggests that the increased potential gradient in the electric field caused an increase in the rate of movement of those counterions to different electrolytes. At the same time, the incorporation of the clay was found to influence strongly the deformation of the hybrid films under an electrical field. As a consequence, the electrostimulus deformation reached equilibrium after 1.5 h of operation. Concerning the deswelling ratio at a time of 1.5 h, as shown in Fig. 6b, the hybrids with lower  $C_{\text{clay}}$  are subjected to smaller restric-

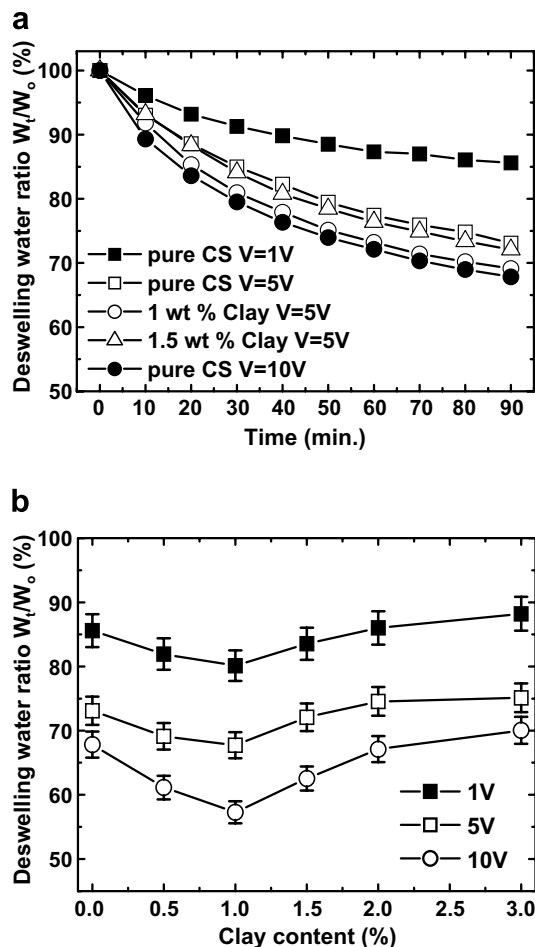


Fig. 6. (a) Deswelling behavior and (b) deswelling water ratio of hybrid film with different  $C_{\text{clay}}$  in a 1.5 h interval under applied voltages of 1, 5 and 10 V.

tions of molecule relaxation than is pure CS. In other words, with increasing  $C_{\text{clay}}$ , the mobility of the hybrid composites was gradually restricted by the formation of an increasing amount of cross-linking bonds. Therefore, the deswelling ratio of the resulting hybrid decreases with increasing  $C_{\text{clay}}$ . As shown in Fig. 6, the hybrid composites containing the lower clay concentration (0.5–1 wt.%) exhibited more rapid responsivity and larger deformation to a given electrical voltage. However, the rate and extent of the deswelling kinetics are both decreased as  $C_{\text{clay}}$  is increased.

### 3.4. Cyclic deformation and recovery of hybrid films

Above a threshold value of a given electrical field, the hybrid film showed deswelling behavior wherein the water is gradually expelled from the hybrid. When the electric field was removed, the matrix swelled by absorbing surrounding water. A repeated on–off operation of the electrical field stimulates the hybrid films with a cyclic swelling–deswelling mechanical deformation. Fig. 7a shows the swelling ratio of the CS film after cyclic on–off

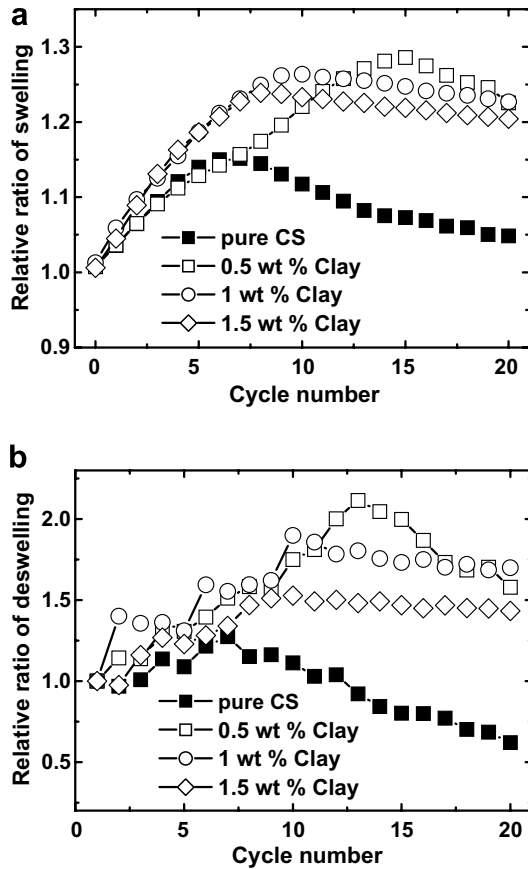


Fig. 7. Relative ratio of (a) swelling and (b) deswelling after cyclic on-off switching of 5 V electrostimuli in a 20 min interval of hybrid films with different  $C_{\text{clay}}$ .

operation of the electrical field in a 20 min interval relative to the original equilibrium swelling ratio of the hybrid film with different clay concentrations under an applied voltage of 10 V. Initially, the equilibrium swelling of pure CS film was increased slightly for several cycles of the on-off operation. This may be due to the collapse of the CS structure under applied voltage and the production of more and more porous structure on the CS film, as was observed visually. The enhanced porosity would improve the degree of swelling to about 1.15 times after six cycles. The degree of swelling would subsequently start to reduce, indicating a fatigue behavior of the CS film. This observation suggests that the CS film should lose its structural integrity after six cyclic operations, thereby causing the CS film to deteriorate by losing its capability of absorbing water. On the contrary, the hybrid composite with lower clay content (0.5 wt.%) showed much better structural integrity, allowing the hybrid to undergo as many as 15 operation cycles, with a higher relative ratio of swelling achievable at about 1.3. The increase in the degree of swelling may be associated with the decrease in the degree of cross-linking caused by the lower  $C_{\text{clay}}$ . However, as the higher concentration of the clay was loaded ( $>0.5$  wt.%), the swelling ratio remained the same when the number of cyclic stimulations exceeded six. In fact, the swelling ratio would not decrease

enormously with increased cyclic stimulation as in the case of pure CS and the hybrid with 0.5 wt.% clay. It is believed that the greater cross-linking density of the hybrid composites is capable of bearing a larger applied voltage and more on-off switching operations. Similarly, the hybrid composites with higher  $C_{\text{clay}}$  ( $>0.5$  wt.%) could maintain the same degree of deswelling after more than 10 operation cycles, compared with the pure CS film and hybrid composites with lower clay content, as shown in Fig. 7b. Hence, the incorporation of clay particles can structurally adjust the cross-linking density of the hybrid and improve the anti-fatigue properties of the hybrids under cyclic electrostimulation.

Fig. 8 shows the weight changes of the pure CS film and the hybrid film (1 wt.% clay) under an applied voltage of 10 V in PBS and consecutive on-off operations in a 20 min interval. For pure CS, the degree of reversibility (i.e., the ability for the hybrid to structurally return to the initial swelling state) is apparently decreased when the on-off operation exceeds seven cycles. Furthermore, the deswelling ratio of the pure CS film could not be restored to the original level after several cyclic operations. The decrease of the swelling and deswelling ratio of the hybrid film can be translated directly as an indication of fatigue behavior of the hybrid. In this study, the films with a composition of 1 wt.% clay showed the best anti-fatigue property where the swelling and deswelling behavior remained identical even after 20 on-off cycles. Since the contractile deformation under stimulation and volume recovery of a given polyelectrolyte hydrogel are associated with the optimal viscoelasticity at a certain cross-linking density, it is suggested that the incorporation of negatively charged clay as a cross-linker provides a more effective anti-fatigue property for pure positively charged chitosan under cyclic electrostimulation. On this base, it is believed that this hybrid is considered in biomedical applications with improved and reliable performance, especially used as drug delivery system which is currently under investigation and will be reported shortly.

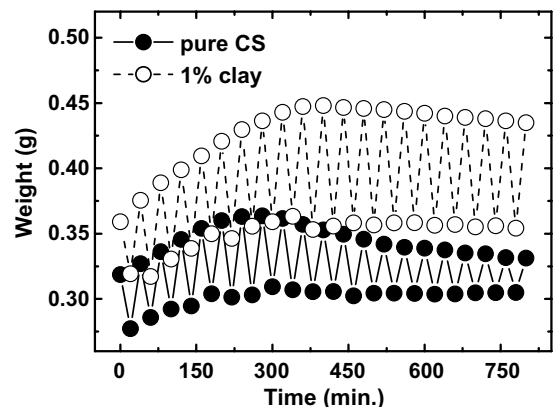


Fig. 8. Weight changes of pure chitosan and hybrid film with 1 wt.% clay addition under cyclic on-off switching of 5 V electrostimuli.

#### 4. Conclusion

An electrostimulus-responsive hybrid composed of chitosan (CS) and clay was successfully prepared and systematically characterized. It was found that the incorporated clay is able to form cross-links with the CS matrix because of the electrostatic interaction between the positively charged  $-\text{NH}_3^+$  group of CS and the negatively charged clay sheets. With considerably increased clay content, this formation of cross-linking reinforces the hybrids and overcomes the adverse effect caused by the small addition of clay. At the same time, the increased cross-linking density improved the mechanical properties of the hybrids, but restricted the swelling–deswelling kinetics. After the repeated switching on and off of a given electric field, a relatively constant swelling–deswelling behavior was achieved for more than 10 cycles for the hybrids with higher  $C_{\text{clay}}$  ( $>0.5$  wt.%), compared with that of the pure CS. The incorporation of the clay not only improved the mechanical strength and anti-fatigue properties under cyclic electrical stimulation of the hybrids, but also imparted the hybrid with a sufficient flexible character to deform in a technically desirable manner under cyclic contraction–expansion. Further investigation of the controlled release profile for a number of clinically valuable drugs using this new class of hybrid composite is underway and will be reported separately.

#### Acknowledgement

This work was financially supported by the National Science Council of the Republic of China, Taiwan under Contract No. NSC-95-2216-E-009-026.

#### References

- [1] Ueoka Y, Gong J, Osada Y. Chemomechanical polymer gel with fish-like motion. *J Intel Mat Syst Str* 1997;8:465–71.
- [2] Feil H, Bae YH, Kim SW. Molecular separation by thermosensitive hydrogel membranes. *J Memb Sci* 1991;64:283–91.
- [3] Kim YH, Bae YH, Kim SW. PH/temperature-sensitive polymers for macromolecular drug loading and release. *J Control Release* 1994;28:143–55.
- [4] Shu XZ, Zhu KJ. Controlled drug release properties of ionically-linked chitosan beads: the influence of anion structure. *Int J Pharm* 2001;212:19–28.
- [5] Gan Q, Wang T, Cochrane C, McCarron P. Modulation of surface charge, particle size and morphological properties of chitosan–TPP nanoparticles intended for gene delivery. *Colloid Surface B* 2005;44:65–73.
- [6] Going JP, Nitta T, Osada Y. Electrokinetic modeling of the contractile phenomena of polyelectrolyte gels. One-dimensional capillary model. *J Phys Chem* 1994;98:9583–7.
- [7] Sutani K, Kaetsu I, Uchida K. The synthesis and the electric-responsiveness of hydrogels entrapping natural polyelectrolyte. *Radiat Phys Chem* 2001;61:49–54.
- [8] Shiga T, Kurauchi T. Deformation of polyelectrolyte gels under the influence of electric field. *J Appl Polym Sci* 1990;39:2305–20.
- [9] Doi M, Matsumoto M, Hirose Y. Deformation of ionic polymer gels by electric fields. *Macromolecules* 1992;25:5504–11.
- [10] Pinnavaia TJ, Beall GW. *Polymer–clay composites*. New York: John Wiley & Sons; 2001.
- [11] Vaia RA, Krishnamoorti R. *Polymer nanocomposites*. Washington, DC: American Chemical Society; 2001.
- [12] Wang SF, Shen L, Tong YJ, Chen L, Phang IY, Lim PQ, et al. Biopolymer chitosan/montmorillonite nanocomposites: preparation and characterization. *Polym Degrad Stabi* 2005;90:123–31.
- [13] Darder M, Colilla M, Ruiz-Hitzky E. Chitosan–clay nanocomposites: application as electrochemical sensors. *Appl Clay Sci* 2005;28:199–208.
- [14] Chen P, Zhang L. Interaction and properties of highly exfoliated soy protein/montmorillonite nanocomposites. *Biomacromolecules* 2006;7:1700–6.
- [15] Haraguchi K, Takegisa T, Fan S. Effects of clay content on the properties of nanocomposite hydrogels composed of poly(*N*-isopropylacrylamide) and clay. *Macromolecules* 2002;35:10162–71.
- [16] Rojo JM, Ruiz-Hitzky E, Sanz J. Proton–sodium exchange in magadiite. Spectroscopic study (NMR, IR) of the evolution of interlayer OH groups. *Inorg Chem* 1988;27:2785–90.
- [17] Bueche F. *Physical properties of polymers*. New York: Wiley; 1962.
- [18] Ludikhuyze LR, Broeck IV, Weemaes CA, Herremans CH, van Impe JF, Hendricks ME. Kinetics for isobaric–isothermal inactivation of *Bacillus subtilis*  $\alpha$ -amylase. *Biotechnol Prog* 1997;13:532–8.
- [19] Ramanathan S, Block LH. The use of chitosan gels as matrices for electrically-modulated drug delivery. *J Control Release* 2001;70:109–23.